

Effects of Observational Data Shortage on Accuracy of Global Solar Activity Forecast

I. N. Kitiashvili^{1,2}

¹*NASA Ames Research Center, Moffett Field, Mountain View, CA 94035, USA*

²*Bay Area Research Environmental Institute, Moffett Field, Mountain View, CA 94035, USA*

ABSTRACT

Building a reliable forecast of solar activity is a long-standing problem that requires to accurately describe past and current global dynamics. However, synoptic observations of magnetic fields and subsurface flows became available relatively recently. In this paper, we present an investigation of effects of short observational data series on accuracy of solar cycle prediction. This analysis is performed using the annual sunspot number time-series applied to the Parker-Kleorin-Ruzmaikin dynamo model and employing the Ensemble Kalman Filter (EnKF) data assimilation method. The testing of the cycle prediction accuracy is performed for the last six cycles (from Solar Cycle 19 to 24) by sequentially shortening the observational data series that are used for prediction of a target cycle, and evaluating the prediction accuracy according to specified criteria. According to the analysis, reliable activity predictions can be made using relatively short time-series of the sunspot number. It demonstrated that even two cycles of available observations allow us to obtain reasonable forecasts.

Subject headings: Sun: photosphere, magnetic fields; Methods: numerical; MHD, plasmas, turbulence

1. Introduction

Forecast of the global solar activity which is usually characterized by sunspot number (SN) variations on the 11-year time scale is a challenging problem due to our limited knowledge about physical processes hidden under the solar surface. A number of approaches that are developed to predict the basic properties of the upcoming solar cycle produced different

¹e-mail: irina.n.kitiashvili@nasa.gov

results (see review by Pesnell 2012) due to uncertainties of models and observations. However, many additional factors affect the prediction accuracy. In particular, it is known that the highest prediction accuracy of upcoming solar cycle can be achieved during the preceding solar minimum (e.g. Svalgaard et al. 2005; Choudhuri et al. 2007; Kitiashvili & Kosovichev 2008, 2011). The solar activity forecast performed during the polar field reversals can also be accurate if the field reversals are synchronized in both hemispheres (Kitiashvili 2016).

There have been many attempts to develop models and data analysis techniques (e.g. Dikpati & Gilman 2007; Cameron & Schüssler 2007; Choudhuri et al. 2007; Kitiashvili & Kosovichev 2008, 2009; Jouve et al. 2011; Karak & Choudhuri 2013; Upton & Hathaway 2014, 2018; Lemerle & Charbonneau 2017; Jiang & Cao 2018; Covas et al. 2019; Macario-Rojas et al. 2018; Labonville et al. 2019) to improve accuracy of the activity forecast and to understand the nature of the global dynamics of the Sun. However, these developments face a problem of observational data shortage that restricts our ability to validate and calibrate a model or analysis approach. In particular, most of the available observations of the surface and atmosphere, such as synoptic magnetograms, solar irradiance, solar faculae, and others cover very few cycles of solar activity (e.g. Muñoz-Jaramillo et al. 2012; Priyal et al. 2014, 2017; Riley et al. 2014; Wu et al. 2018). Inferences of the subsurface dynamics cover only the last two sunspot cycles (e.g. Zhao & Kosovichev 2004; Zhao et al. 2013; Komm et al. 2018; Kosovichev & Rozelot 2018; Kosovichev & Pipin 2019; Liang et al. 2018; Howe et al. 2018).

In this paper, we take advantage of over 400-years sunspot number time-series to investigate effects of short data series on the accuracy of the solar cycle prediction. We perform test predictions for the solar cycles from Cycle 19 (SC19) to Cycle 24 (SC24). In the next section, we describe the annual sunspot number data series used in the analysis. Sections 3 and 4 include a brief description of the Parker-Kleorin-Ruzmaikin (PKR) mean-field dynamo model and methodology. Section 5 presents reconstructions for the six target cycles using the sunspot number observations of different lengths preceding these cycles. We discuss accuracy of the predictions in Section 6, and summarize conclusions in Section 7.

2. Sunspot number time-series

We use the annual sunspot number time-series data (version 2.0, Fig. 1) from the WDC-SILSO¹ repository of the Royal Observatory (Brussels, Belgium). According to our previous studies, the different calibrations (or version) of the sunspot number series do not affect the analysis results after applying the corresponding observational data rescaling (Kitiashvili

¹<http://www.sidc.be/silso/datafiles>

2016).

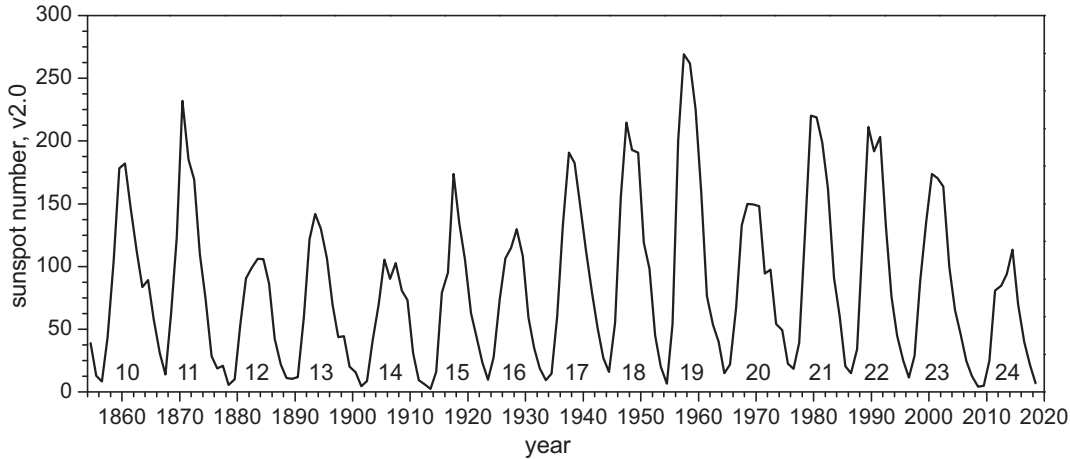


Fig. 1.— The annual sunspot number (v2.0) time-series from the WDC-SILSO repository of the Royal Observatory (Brussels, Belgium).

3. Mean-field dynamo model

For the data assimilation procedure, we use the mean-field dynamo model described by Kitiashvili & Kosovichev (2008, 2009), in which the Parker’s migratory $\alpha\Omega$ -dynamo model (Parker 1955) is combined with the equation of magnetic helicity balance (Kleeorin & Ruzmaikin 1982; Kleeorin et al. 1995). It has been shown that taking into account the evolution of the magnetic helicity provides an explanation of the Waldmeier’s relations (Kitiashvili & Kosovichev 2008; Pipin & Kosovichev 2011). In a simplified form, the dynamo model is described by the following equations:

$$\begin{aligned}
 \frac{\partial A}{\partial t} &= \alpha B + \eta \nabla^2 A \\
 \frac{\partial B}{\partial t} &= G \frac{\partial A}{\partial x} + \eta \nabla^2 B, \\
 \frac{\partial \alpha_m}{\partial t} &= -\frac{\alpha_m}{T} + \frac{Q}{4\pi\rho} \left[\langle \mathbf{B} \rangle \cdot (\nabla \times \langle \mathbf{B} \rangle) - \frac{\alpha}{\eta} \langle \mathbf{B} \rangle^2 \right],
 \end{aligned}
 \tag{1}$$

where A and B are the vector-potential and the toroidal field component of magnetic field \mathbf{B} , $\alpha = \alpha_h + \alpha_m$ is total helicity, which includes the hydrodynamic helicity (α_h), and magnetic helicity (α_m) parts, η is total magnetic diffusion, which includes the turbulent and molecular magnetic diffusivity, $\eta = \eta_t + \eta_m$ (usually $\eta_m \ll \eta_t$), G describes the rotational

shear, ρ is density, Q and T are coefficients which describe characteristic scales and times (Kleeorin & Ruzmaikin 1982), x is radial coordinate, and t is time.

To perform the data assimilation analysis, we employ a low-mode approximation (Weiss et al. 1984), which reduces the mean-field Parker-Kleeorin-Ruzmaikin (PKR) dynamo model (Eq. 1) to a non-linear dynamical system (Kitiashvili & Kosovichev 2009; Kitiashvili 2019)

$$\begin{aligned} \frac{dA}{dt} &= DB - A, & \frac{dB}{dt} &= iA - B, \\ \frac{d\alpha_m}{dt} &= -\nu\alpha_m - D [B^2 - \lambda A^2], \end{aligned} \quad (2)$$

where A , B , α_m and t are non-dimensional variables, $D = D_0\alpha$ is the non-dimensional dynamo number, $D_0 = \alpha_0 Gr^3/\eta^2$, $\alpha_0 = 2Qkv_A^2/G$, v_A is the Alfvén speed, $\lambda = (k^2\eta/G)^2 = \text{Rm}^{-2}$, k is a characteristic wavelength, $\nu \sim 2k_0\eta_m^2/(k^2\eta t)$, k_0 is largest scale in the inertial range of the turbulence spectrum (Kleeorin & Ruzmaikin 1982).

Despite the simple formulation, the model describes the basic features of the solar cycles: generation and transformation of the poloidal and toroidal magnetic field components as well as the evolution of the sunspot number, W , which is modeled following the Bracewell’s relation $W = \text{const}B^{3/2}$. Previous studies demonstrated the ability of the mean-field PKR model to reproduce the qualitative properties of the solar cycles (Kitiashvili & Kosovichev 2009) that makes the model suitable for application of the Ensemble Kalman Filter. In this paper, assimilation of the sunspot number time series is performed using the model solutions, which have been obtained for the following parameters: $\alpha_k = 1.8$, $D_0 = -3.3$, $\nu = 0.013$, $\lambda = 3.2 * 10^{-6}$, and $q = 5.87$.

4. Assimilation of sunspot number time series into the PKR dynamo model using Ensemble Kalman Filter

The previous successful application of the data assimilation approach (Kitiashvili & Kosovichev 2008), and, in particular, the Ensemble Kalman Filter method (EnKF, Evensen 1994) can be explained by the following factors: 1) the derived mean-field dynamo model is able to reproduce the general properties of the sunspot cycles; 2) the model and assimilated data correspond to each other in terms of complexity and robustness; 3) the availability of long data-series of the sunspot number is critical for the model calibration and estimation of observational uncertainties. According to the dynamo theory (Babcock 1961; Leighton 1969), active regions represent toroidal magnetic fields generated in the solar interiors as a result of the differential rotation. Qualitative relationship between the toroidal magnetic field component and the sunspot number, $W = \text{const}B^{3/2}$ (where W is the sunspot number, and B

is the toroidal field component) suggested by Bracewell (1988) provides a link between the sunspot number time series and the general global field variations. In this paper, we use this relationship to assimilate the available sunspot number time-series into the reduced dynamo model (Eq. 2). For performing the EnKF analysis, the periodic model solution is normalized to the strength of the last observed solar cycle in our test series. In a case of the phase discrepancy between the model and data by two or more years, the model solution is shifted to get a better phase agreement of the solar cycle minimum times. Synthetic observations of the poloidal field and magnetic helicity are generated from the model solution with added random noise of 10%.

5. Tests of the solar cycle prediction using limited amount of sunspot data

To investigate the influence of short observational data series, we perform a series of test predictions for six solar cycles from 19 to 24. Including SC19 and SC21 allows us to test the ability to predict transition to stronger activity cycles. We perform the test predictions by assimilating from nine to two cycles of sunspot observations and using 300 ensemble members in the EnKF procedure. For instance, for the test prediction of Solar Cycle 19 (SC19), we use initially nine cycles-long time-series of the sunspot number (from SC10 to SC18). Then, we remove from the analysis procedure the sunspot number observations, cycle-by-cycle, starting from SC10, and sequentially evaluating the cycle prediction accuracy.

The performed prediction tests led us to the following criteria to examine the quality of the obtained solar activity predictions in the descending order of importance:

1. the phase discrepancy between the exact model solution and observations should not be greater than 2 years;
2. if at the end of the reconstruction phase the exact solution of the toroidal magnetic field component is about zero, it can be considered as an evidence of high prediction accuracy;
3. the signs of the last available observation (for the toroidal field) and the corresponding model solution should be same; however, if the last observational data point is too far from the solar minima it can significantly reduce the forecast accuracy;
4. the exact model solution for the prediction phase must be consistent with the model solution for the reconstruction phase (the solution should not be with extreme flattening, or exhibit jumps or ‘bumps’, but the solution may be shifted according to new initial condition); and

5. the corrected solution (first guess estimate) at the initial moment of time during the prediction phase should not be greater than the best-estimate variations of the toroidal field. This criterion provides only a suggestion about the possibility of an inaccurate prediction, therefore it is applicable if the previous criteria are satisfied.

The criteria to evaluate the accuracy of a forecast are defined from the prediction performance that was obtained for the different lengths of the observational time-series. The forecasts are rated as accurate if the maximum sunspot number is predicted with the amplitude error not exceeding 15% and the time error not exceeding 1 year.

The first three criteria are most important for the evaluation of a prediction. The first criterion was previously identified by Kitiashvili & Kosovichev (2008). The second one comes from the previously found importance of setting up the initial conditions to perform a prediction of the upcoming activity during the periods of a high ratio between the toroidal and poloidal magnetic field components (Kitiashvili 2016). The third criterion intends to capture potentially strong discrepancies between the model solutions and the last available observation of the toroidal field. The fourth criterion captures abnormal behavior of the non-linear solution in the rising phase of the predicted cycle, such as the appearance of unexpected fluctuations of the toroidal field. The last, fifth criterion can be used only if several prediction results more or less similarly satisfy the previous four criteria, and provide a broad range of the predicted cycle properties. This primarily happens if the observational time series are only 2 – 3 solar cycles long.

According to the study, the most efficient approach in obtaining an accurate forecast includes the following steps:

- Perform a test forecast of a past cycle to calibrate phases of the periodic model solution and preceding solar activity to obtain agreement between the predicted and actual cycle properties.
- Repeat the previous analysis to perform prediction of the next cycle by using the information about the model periodic solution phase. If the discrepancy between the last observed cycle and the model solution is more than two years, shift the model solution by one year.

Previously, this sequential approach has been used to predict Solar Cycle 24 (Kitiashvili & Kosovichev 2008).

Following the criteria described above, the test prediction results and the corresponding solutions for the toroidal magnetic field component for Solar Cycles 19 – 24 for the different

length of the sunspot time series are collected in the graphical form in Appendix. Below we review the prediction accuracy for each of the six test cycles.

Solar Cycle 19 is the strongest in the test series. The predicted and observed SC19 sunspot number are in agreement when the EnKF analysis includes the sunspot time-series of 9, 7 and 4 cycles long (Fig. 2). Evaluation of the toroidal field variations (Fig. 3) in most cases shows the same sign for both, the last observed toroidal field (estimated from the sunspot number according to the Hale law) and the model solution (black lines). According to the above criteria, the obtained predictions are likely to be accurate. However, only three of eight test predictions have good agreement with the actual observations.

Solar Cycle 20 is significantly weaker than SC19. In the forecast, the previous prediction results for SC19 have been taken into account. For instance, for the prediction of SC20, in which the observational data set was 5-cycles long, the phase of the periodic model solution was taken from the prediction of SC19, which was obtained with 4-cycles of observations and was accurate. In most cases, the predicted accuracy of SC20 forecast based on the properties of the toroidal field variations (Fig. 5), corresponds to the actual observations (Fig. 4). There were only three predictions wrongly rated by our a priori criteria as accurate. Nevertheless, the rising phase of the solar activity up to the solar maximum was reproduced correctly in these cases.

Solar Cycle 21 is 50 % stronger than the previous cycle, SC20. According to the forecast accuracy criteria, seven of the eight test predictions were expected to be accurate. However one test, when two cycles of observation were used, was rated as not sufficiently accurate. Nevertheless, even in this case, the prediction results follow the actual sunspot data. It is important to note that in some cases, which are rated as accurate, according to defined criteria, may be noticeable discrepancies in the toroidal field and sunspot observations during the rising phase of the solar activity (Fig. 6, 7). In this and following analysis, we used our test results for predictions of the previous cycles.

Prediction for **Solar Cycle 22** showed performance similar to SC21. All forecasts were expected to provide accurate estimations of the strength and time of the solar maximum (Fig. 9). However, in the test case with 4 preceding cycles, the solar activity during SC22 was underestimated by 23% (Fig. 8).

Solar Cycle 23 followed the trend of the long-term decreasing global activity and was weaker of the previous cycle by 20%. Evaluation of the toroidal field evolution allowed us to identify correctly all accurate and inaccurate predictions (Figs. 10, 11).

Solar Cycle 24 is the weakest in considered time-series with the maximum sunspot number of about 60% smaller of the previous activity cycle. The forecast quality control

correctly identified 5 accurate and one inaccurate predictions. Two cases of the overestimated cycle strengths (by 31% and 22%) were identified correctly.

6. Discussion

Future development of tools for solar activity prediction requires understanding of limitations caused by availability of short time-series of observational data. The first step in this direction is performed in this study, in which the sunspot number series of various length are assimilated into simplified dynamo model using the EnKF method. The test prediction results for the last six cycles using the different length of the preceding sunspot number data-series are presented in Section 5 and Appendix. In this study, the sunspot number is converted into the toroidal magnetic field component following to the three-halves law suggested by Bracewell (1988) with proper scaling and sign definition according to the Hale’s law. However, there is some freedom to choose which observations are considered as the first and last in the observational data set. Thus, in this situation it is possible to obtain several forecasts for about the same amount of observational data, which raises the question about the ranking of these predictions to choose the best one.

We rank our test predictions using the criteria listed in the previous section. These tests are evaluated for the forecast accuracy, thus for our ability to evaluate if the predicted strength of a target cycle is correct. Thus, if according to our criteria we expect that our prediction results is accurate, and if the predicted sunspot maximum indeed deviates from the observed value by less than 15%, we consider this test result as true positive (TP). If we expect an accurate prediction, but predicted maximum of the sunspot number deviates from the actual data by more than 15%, than the test case is identified as false positive (FP). Similarly, if the obtained solution does not follow our first three criteria, we consider this forecast as inaccurate. However, if the comparison of the predicted cycle strength with the actual sunspot maximum is less than 15 %, the test case is ranked as false negative (FN). Similarly, we define the test as true negative (TN) for larger discrepancies between the prediction and observations. A statistical representation of the performance is shown in Table 1. Also, it is useful to include combinations of these scores such as *Accuracy* $((TP+TN)/(TP+FP+FN+TN))$, *Precision* $(TP/(TP+FP))$, *Recall* $(TP/(TP+FN))$, and *F1-score* $(2 \times \text{Precision} \times \text{Recall} / (\text{Precision} + \text{Recall}))$.

As shown in Table 1, the *accuracy* of the prediction is the lowest for SC19 when no additional knowledge about the correspondence between the modeled and observed activity phases was used. Therefore, the increasing accuracy for the other target cycles is expected because the previous tests with assimilation about the same amount of observational data

Table 1: Performance metrics of solar activity forecasts.

	SC19	SC20	SC21	SC22	SC23	SC24
TP	3	5	7	7	7	5
TN	1	0	0	0	1	1
FP	4	3	0	1	0	2
FN	0	0	1	0	0	0
Accuracy	0.500	0.625	0.875	0.875	1.000	0.625
Precision	0.429	0.625	1.000	0.875	1.000	0.714
Recall	1.000	1.000	0.875	1.000	1.000	1.000
F1-score	0.600	0.769	0.933	0.933	1.000	0.833

allowed us to better calibrate our model. The *precision* characteristic, which means the ability to identify accurate predictions, also increases as we accumulate more information during the test predictions for the previous cycles. The *recall* characteristic describes the ability to point all correct predictions, shows a good performance for all target cycles. Concerning the test results with assimilation of observational data only up to four preceding cycles, it is important to note that the incorrect rating of the forecast accuracy were only in three cases: the false-positive prediction of SC19 using two preceding solar cycles, the false-negative forecast for SC21 also using two cycles of observations, and the false-positive prediction of SC22 with 4 preceding cycles of observations. The overall performance of our test predictions suggests that short time-series of observations can be successfully applied to make a reliable forecast.

7. Conclusions

The data assimilation approach to combine a global dynamo-model with the annual sunspot number through the Ensemble Kalman Filter method has demonstrated a great potential to make a reliable forecast for the solar activity cycles. Further development of new physics-based capabilities to predict solar activity on the global scales requires assimilation of synoptic observations, such as magnetic fields, in more detailed dynamo models. This raises a question about the dependence of the forecast accuracy on the length of available observational data series. In this paper, we used the annual sunspot number to test the possibility to perform a reliable forecast for short time-series of observational data, and develop a methodology to evaluate the accuracy of the obtained prediction. A series of tests to predict the solar activity for six target cycles for different lengths of the observed

time-series showed the ability to build reliable long-term activity forecasts. In this work, the criteria to evaluate the forecast accuracy were developed. While the performed analysis demonstrates a good capability to produce a reliable forecast for stronger and weaker cycles, it also showed the importance of long time-series of observations. Longer time-series allow us to perform test predictions for the optimal choice of the model parameters, and estimate the model uncertainty. In the following paper, we expand this study to analysis of the synoptic magnetograms, which are available for the last four cycles of solar activity (Kitiashvili 2019). The next step will include development of the data assimilation analysis for 2D observational data and more detailed dynamo model.

Acknowledgment. The work is supported by NSF grant AGS-1622341.

REFERENCES

- Babcock, H. W. 1961, *ApJ*, 133, 572
- Bracewell, R. N. 1988, *MNRAS*, 230, 535
- Cameron, R., & Schüssler, M. 2007, *ApJ*, 659, 801
- Choudhuri, A. R., Chatterjee, P., & Jiang, J. 2007, *Physical Review Letters*, 98, 131103
- Covas, E., Peixinho, N., & Fernandes, J. 2019, *Sol. Phys.*, 294, 24
- Dikpati, M., & Gilman, P. A. 2007, *New Journal of Physics*, 9, 297
- Evensen, G. 1994, *J. Geophys. Res.*, 99, 10
- Howe, R., Chaplin, W. J., Davies, G. R., et al. 2018, *MNRAS*, 480, L79
- Jiang, J., & Cao, J. 2018, *Journal of Atmospheric and Solar-Terrestrial Physics*, 176, 34
- Jouve, L., Brun, A. S., & Talagrand, O. 2011, *ApJ*, 735, 31
- Karak, B. B., & Choudhuri, A. R. 2013, *Research in Astronomy and Astrophysics*, 13, 1339
- Kitiashvili, I., & Kosovichev, A. G. 2008, *ApJ*, 688, L49
- Kitiashvili, I. N. 2016, *ApJ*, 831, 15
- . 2019, arXiv e-prints, arXiv:1910.00820
- Kitiashvili, I. N., & Kosovichev, A. G. 2009, *Geophysical and Astrophysical Fluid Dynamics*, 103, 53

- Kitiashvili, I. N., & Kosovichev, A. G. 2011, in *Lecture Notes in Physics*, Berlin Springer Verlag, Vol. 832, *Lecture Notes in Physics*, Berlin Springer Verlag, ed. J.-P. Rozelot & C. Neiner, 121
- Kleeorin, N., Rogachevskii, I., & Ruzmaikin, A. 1995, *A&A*, 297, 159
- Kleeorin, N. I., & Ruzmaikin, A. A. 1982, *Magnetohydrodynamics*, 18, 116
- Komm, R., Howe, R., & Hill, F. 2018, *Sol. Phys.*, 293, 145
- Kosovichev, A., & Rozelot, J.-P. 2018, *ApJ*, 861, 90
- Kosovichev, A. G., & Pipin, V. V. 2019, *ApJ*, 871, L20
- Labonville, F., Charbonneau, P., & Lemerle, A. 2019, *Sol. Phys.*, 294, 82
- Leighton, R. B. 1969, *ApJ*, 156, 1
- Lemerle, A., & Charbonneau, P. 2017, *ApJ*, 834, 133
- Liang, Z.-C., Gizon, L., Birch, A. C., Duvall, T. L., & Rajaguru, S. P. 2018, *A&A*, 619, A99
- Macario-Rojas, A., Smith, K. L., & Roberts, P. C. E. 2018, *MNRAS*, 479, 3791
- Muñoz-Jaramillo, A., Sheeley, N. R., Zhang, J., & DeLuca, E. E. 2012, *ApJ*, 753, 146
- Parker, E. N. 1955, *ApJ*, 122, 293
- Pesnell, W. D. 2012, *Sol. Phys.*, 281, 507
- Pipin, V. V., & Kosovichev, A. G. 2011, *ApJ*, 741, 1
- Priyal, M., Banerjee, D., Karak, B. B., et al. 2014, *ApJ*, 793, L4
- . 2017, *VizieR Online Data Catalog*, 179
- Riley, P., Ben-Nun, M., Linker, J. A., et al. 2014, *Sol. Phys.*, 289, 769
- Svalgaard, L., Cliver, E. W., & Kamide, Y. 2005, in *Astronomical Society of the Pacific Conference Series*, Vol. 346, *Large-scale Structures and their Role in Solar Activity*, ed. K. Sankarasubramanian, M. Penn, & A. Pevtsov, 401
- Upton, L., & Hathaway, D. H. 2014, *ApJ*, 780, 5
- Upton, L. A., & Hathaway, D. H. 2018, *Geophys. Res. Lett.*, 45, 8091

Weiss, N. O., Cattaneo, F., & Jones, C. A. 1984, *Geophysical and Astrophysical Fluid Dynamics*, 30, 305

Wu, C.-J., Krivova, N. A., Solanki, S. K., & Usoskin, I. G. 2018, *A&A*, 620, A120

Zhao, J., Bogart, R. S., Kosovichev, A. G., Duvall, Jr., T. L., & Hartlep, T. 2013, *ApJ*, 774, L29

Zhao, J., & Kosovichev, A. G. 2004, *ApJ*, 603, 776

A. Appendix. Results of the test predictions described in Section 5

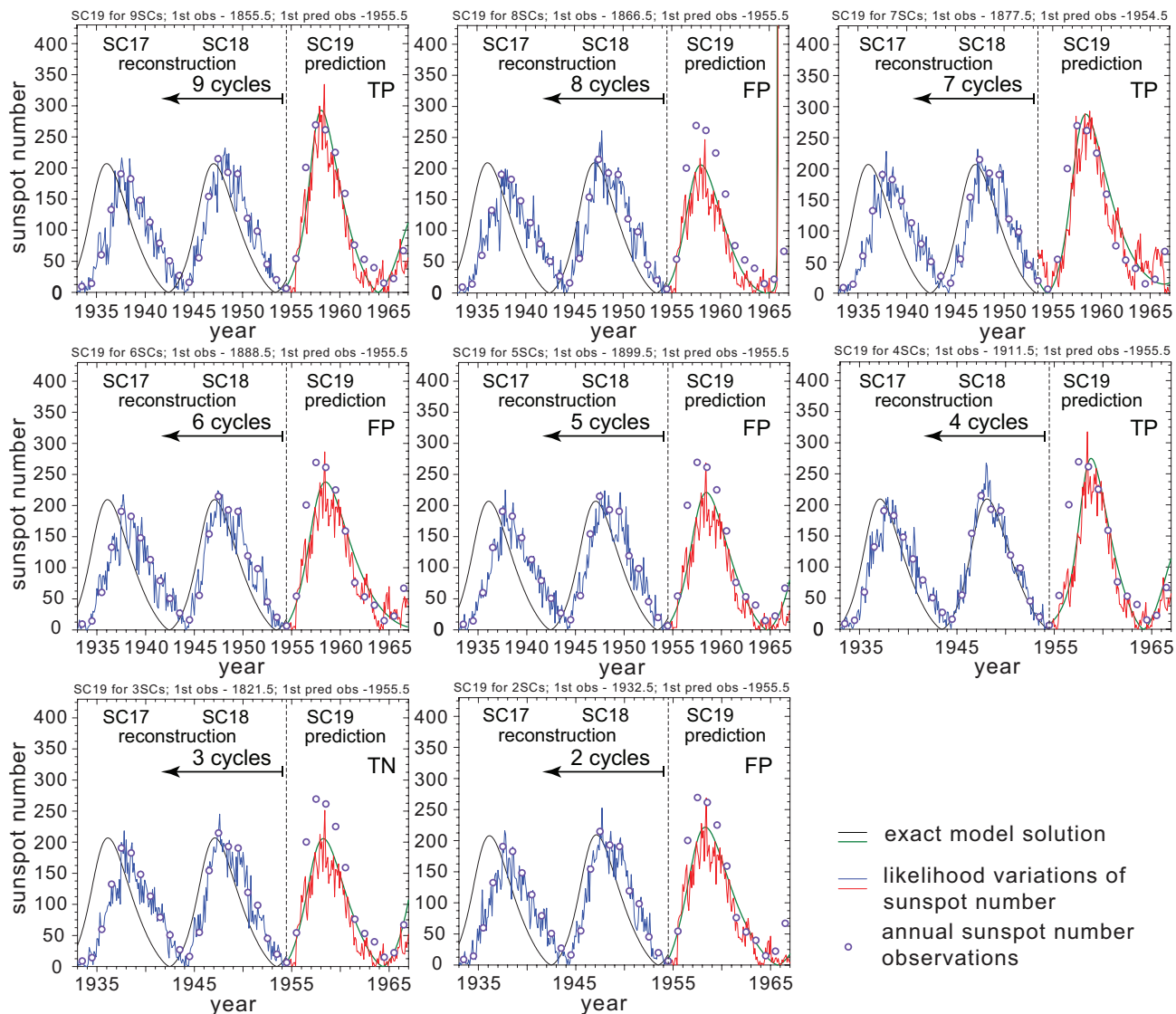


Fig. 2.— The test predictions of Solar Cycle 19 using the preceding sunspot number series of different length, from 9 solar cycles to 2 solar cycles. Black and green curves show exact model solutions at the reconstruction and prediction phases. Blue and red curves correspond to the likelihood variations of the sunspot number. The actual annual sunspot number indicated by circles.

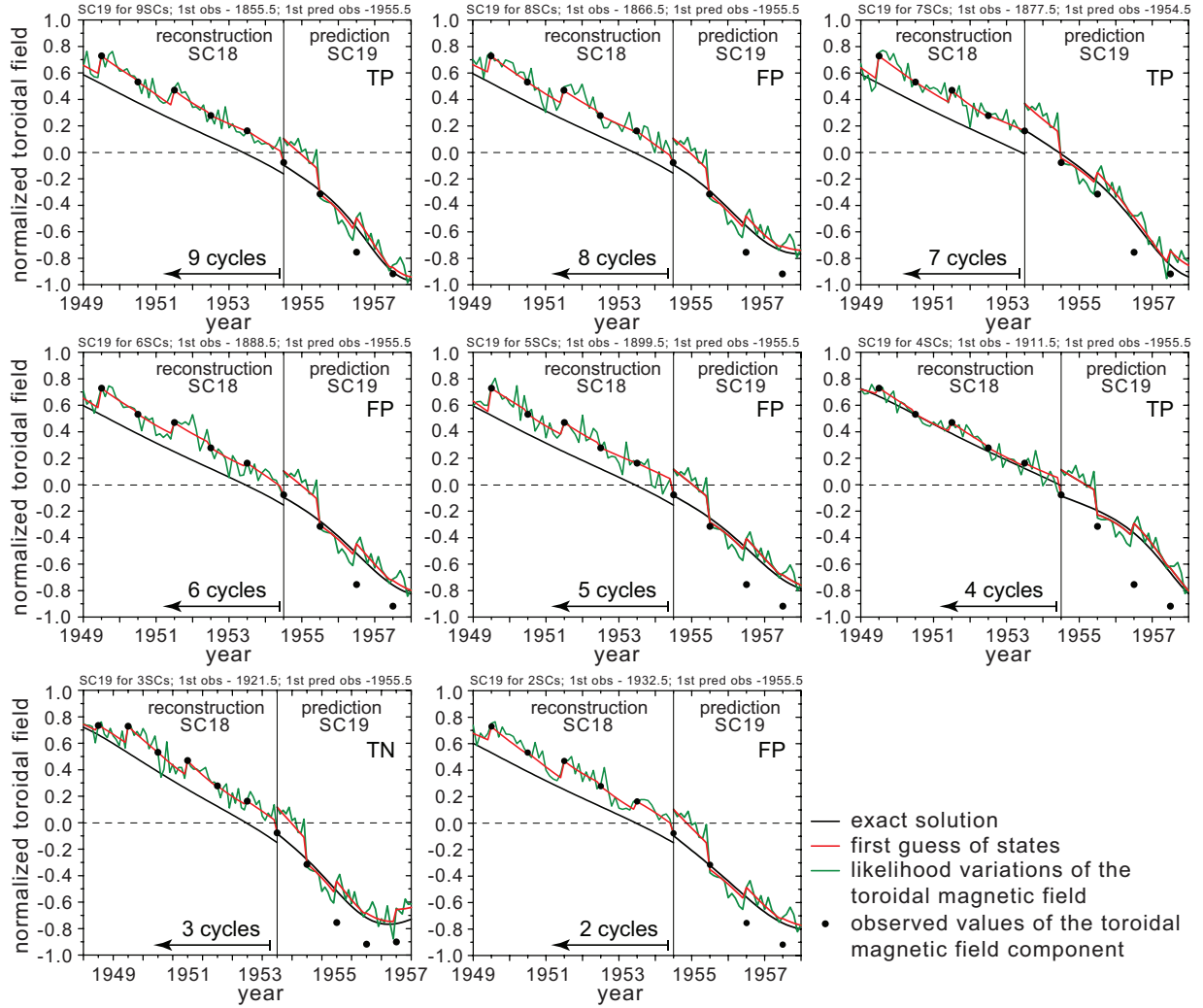


Fig. 3.— Magnified solutions of the toroidal magnetic field to predict Solar Cycle 19 at the end of the reconstruction and the beginning of the prediction phases. Red curves indicate the corrected model solution (black curves), so-called also as the first guess, according to observations the toroidal component of the magnetic field (dots).

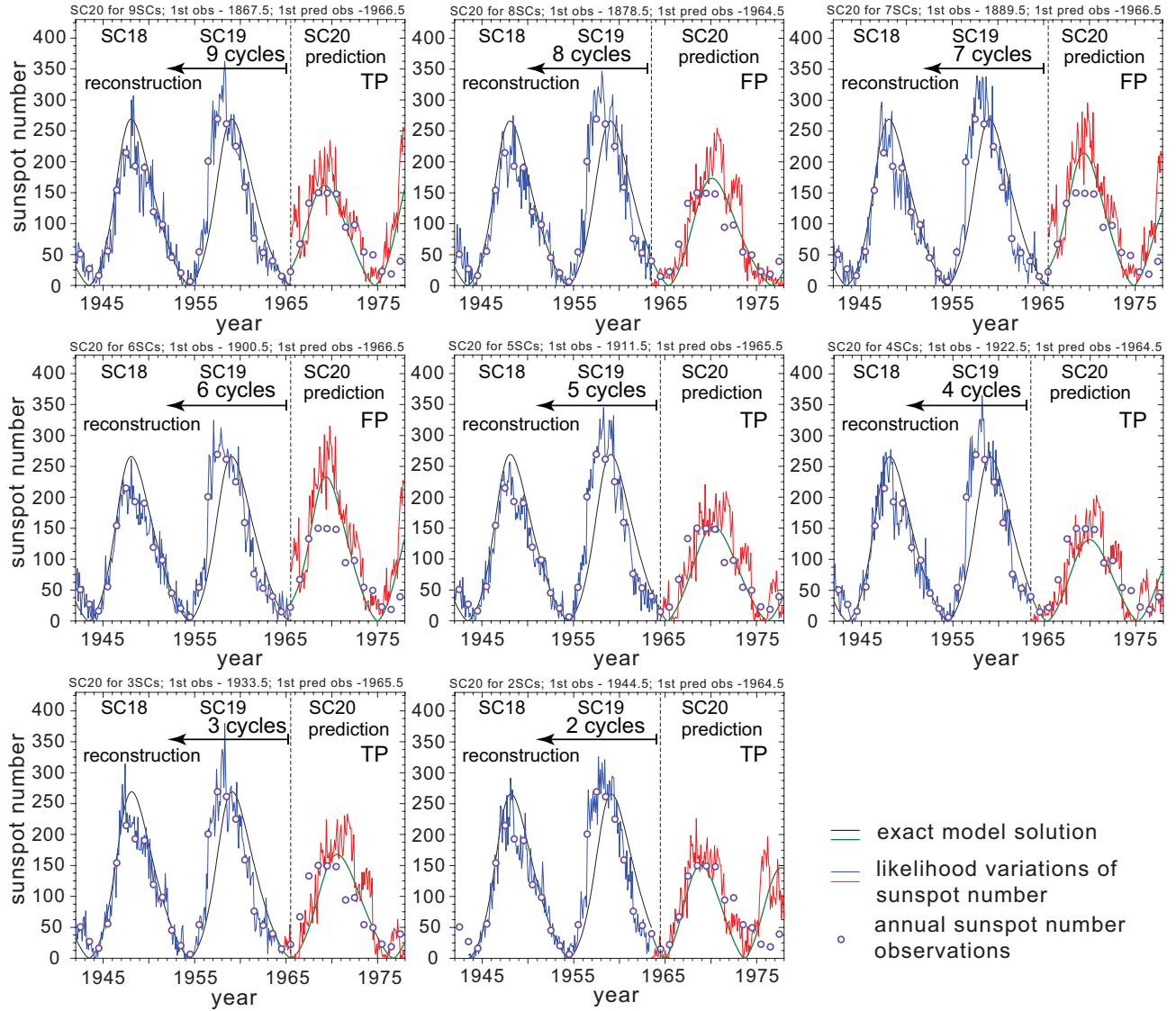


Fig. 4.— The same as in Figure 2 for Solar Cycle 20.

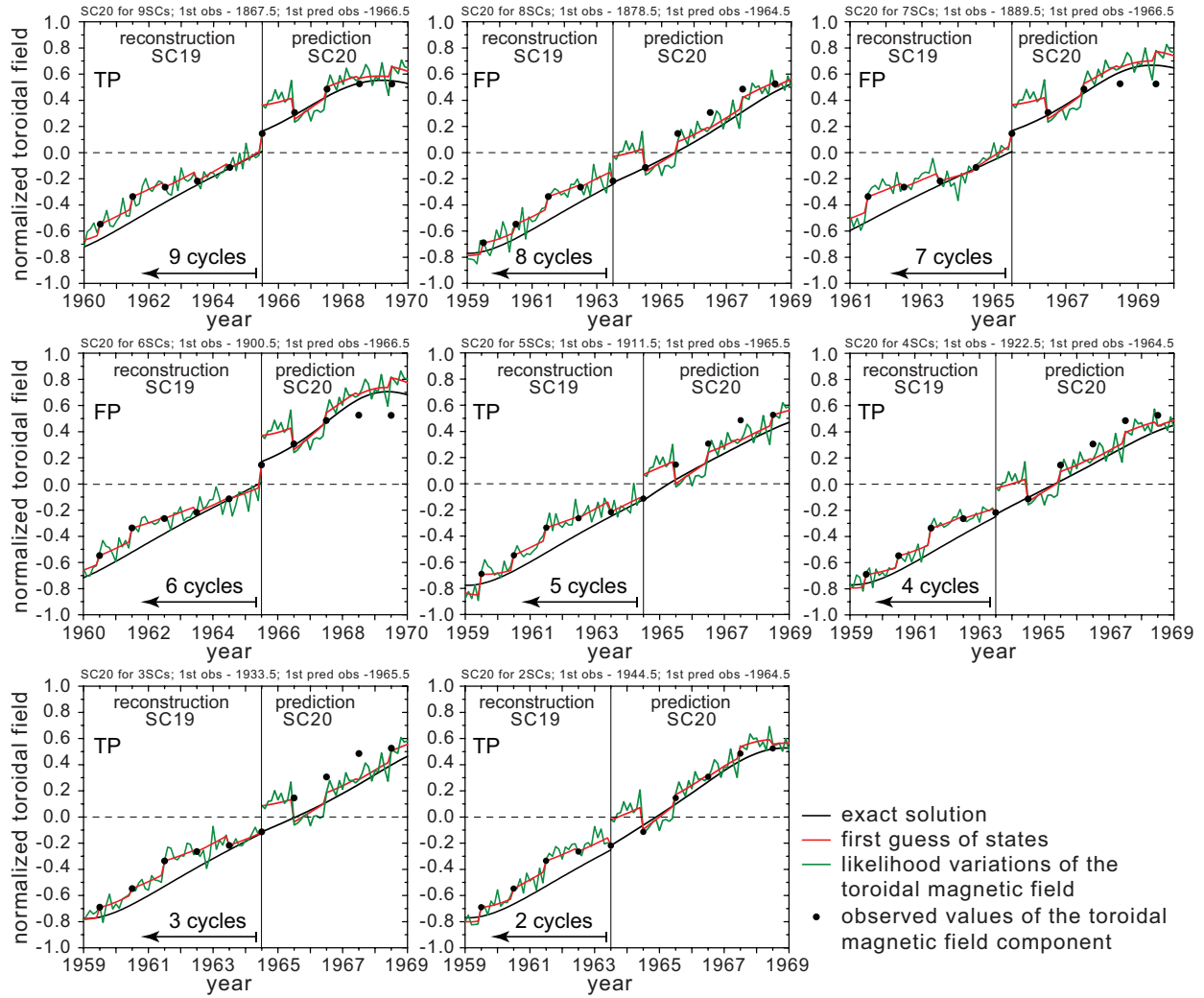


Fig. 5.— The same as in Figure 3 for Solar Cycle 20.

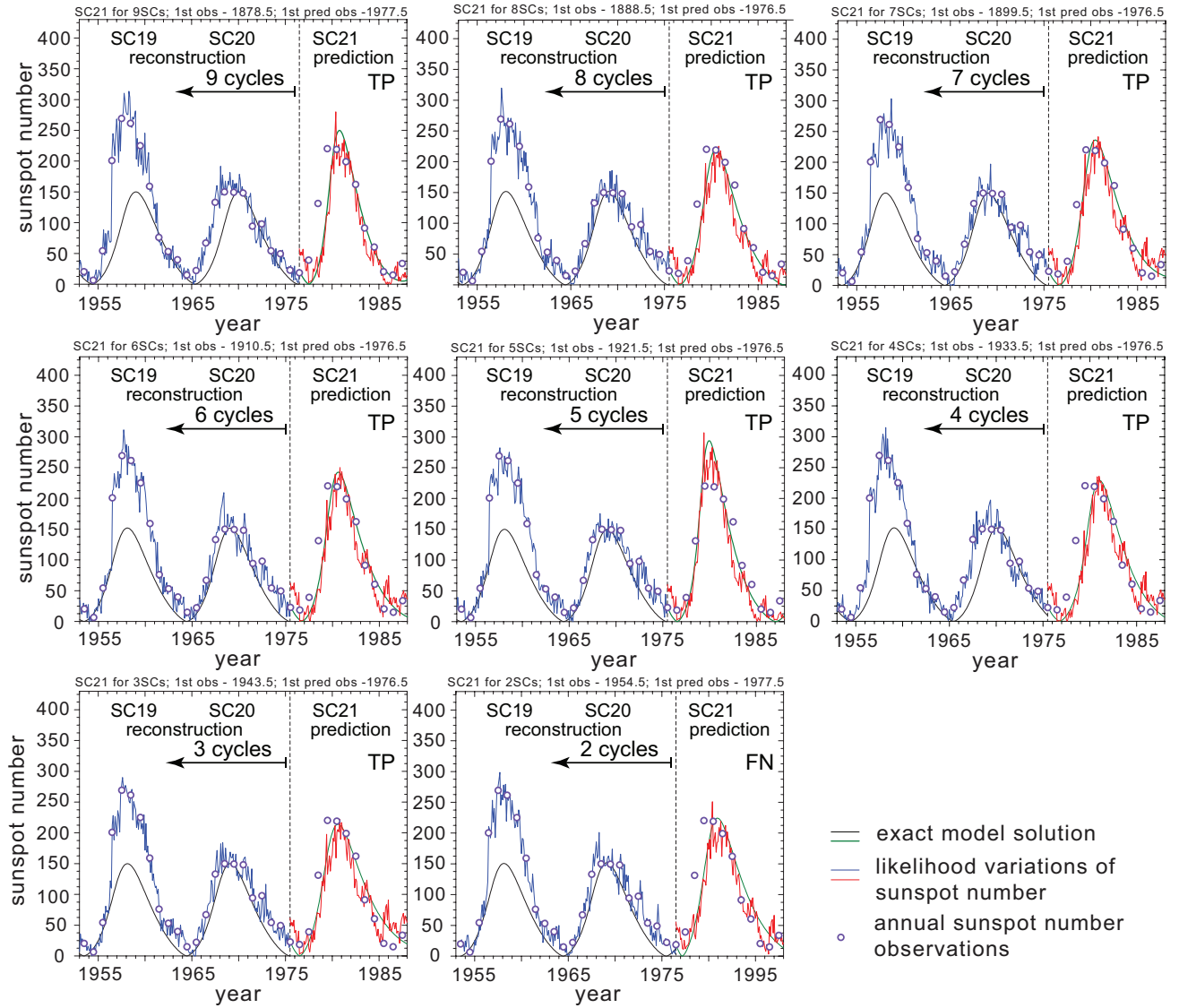


Fig. 6.— The same as in Figure 2 for Solar Cycle 21.

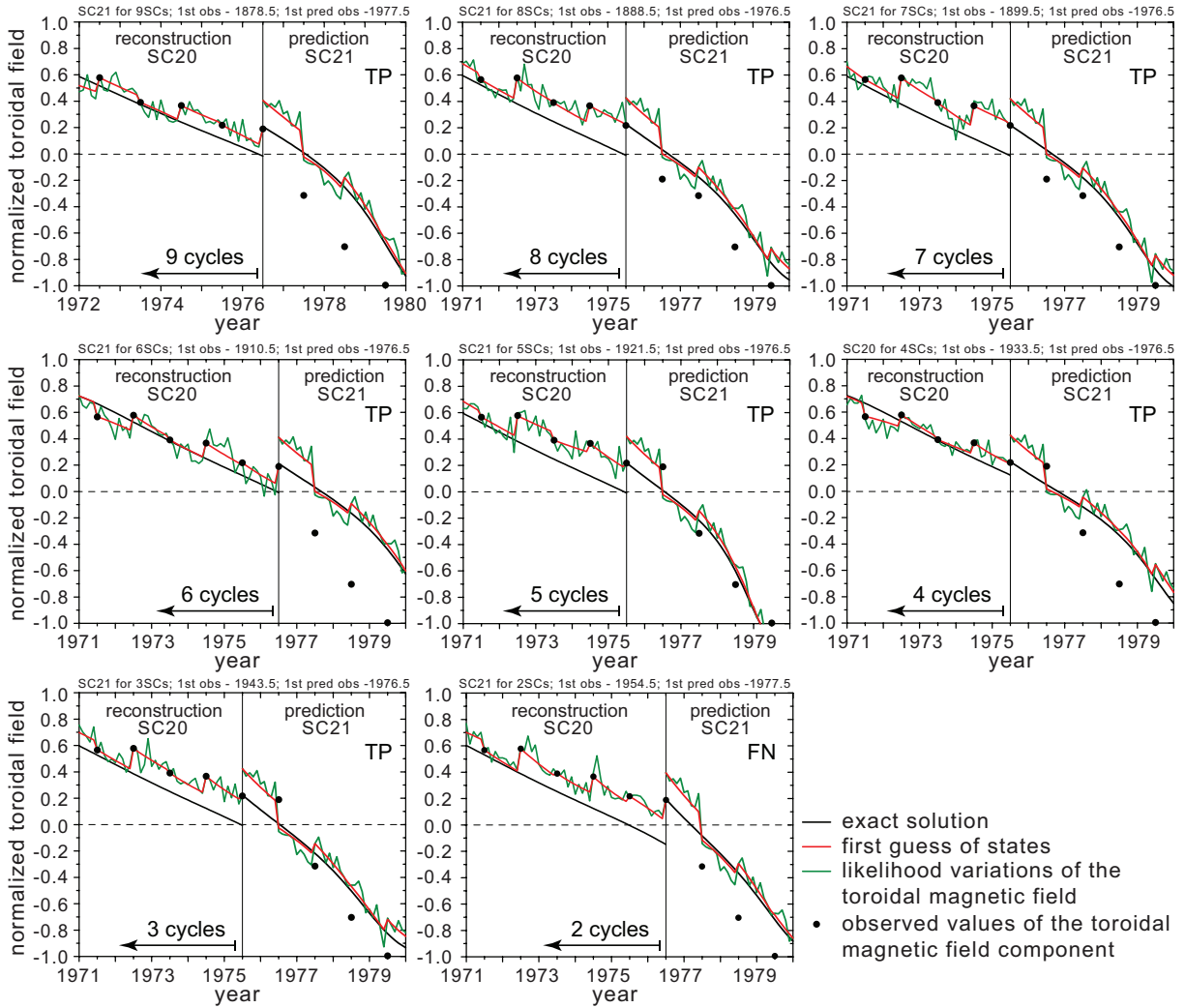


Fig. 7.— The same as in Figure 3 for Solar Cycle 21.

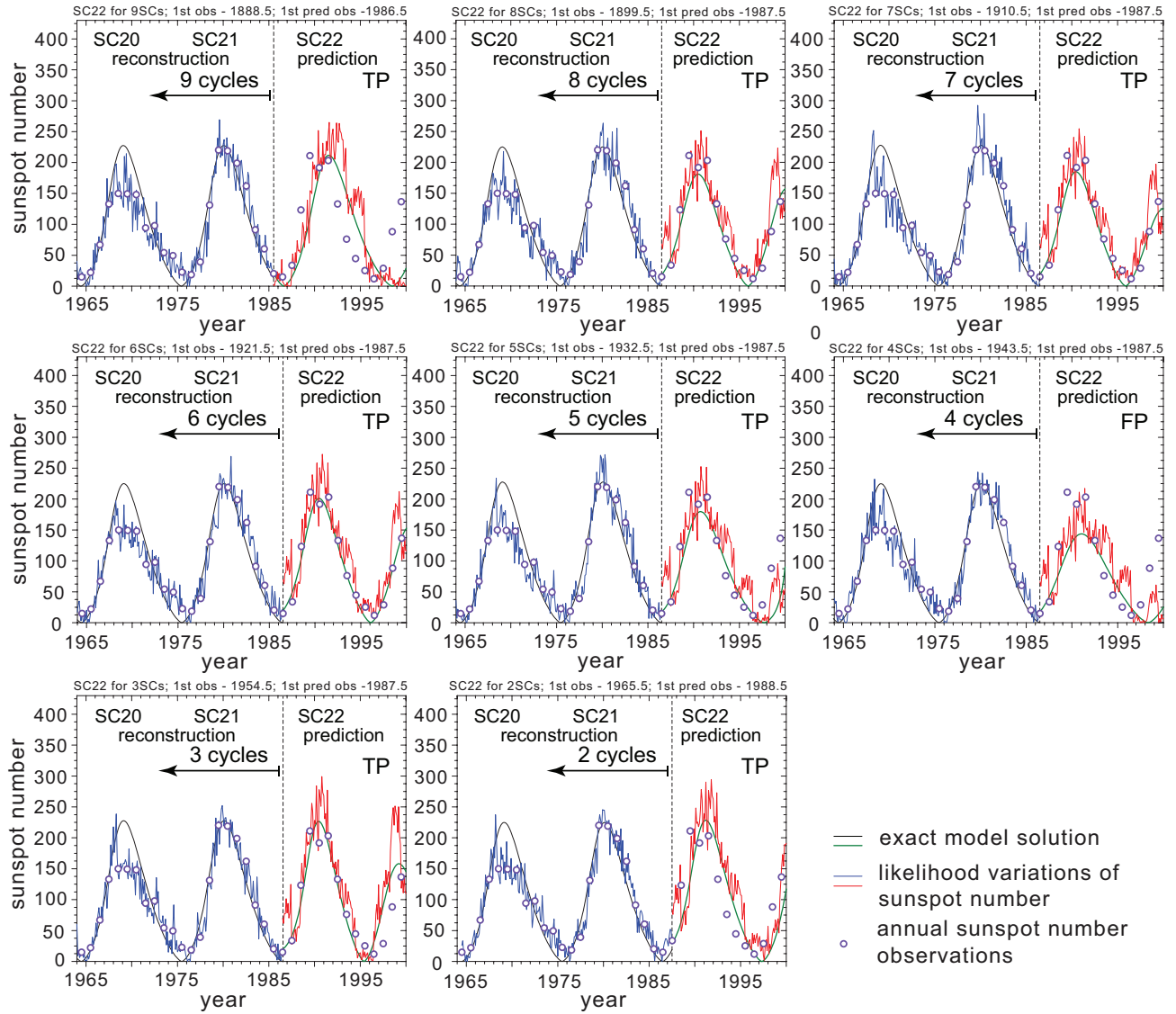


Fig. 8.— The same as in Figure 2 for Solar Cycle 22.

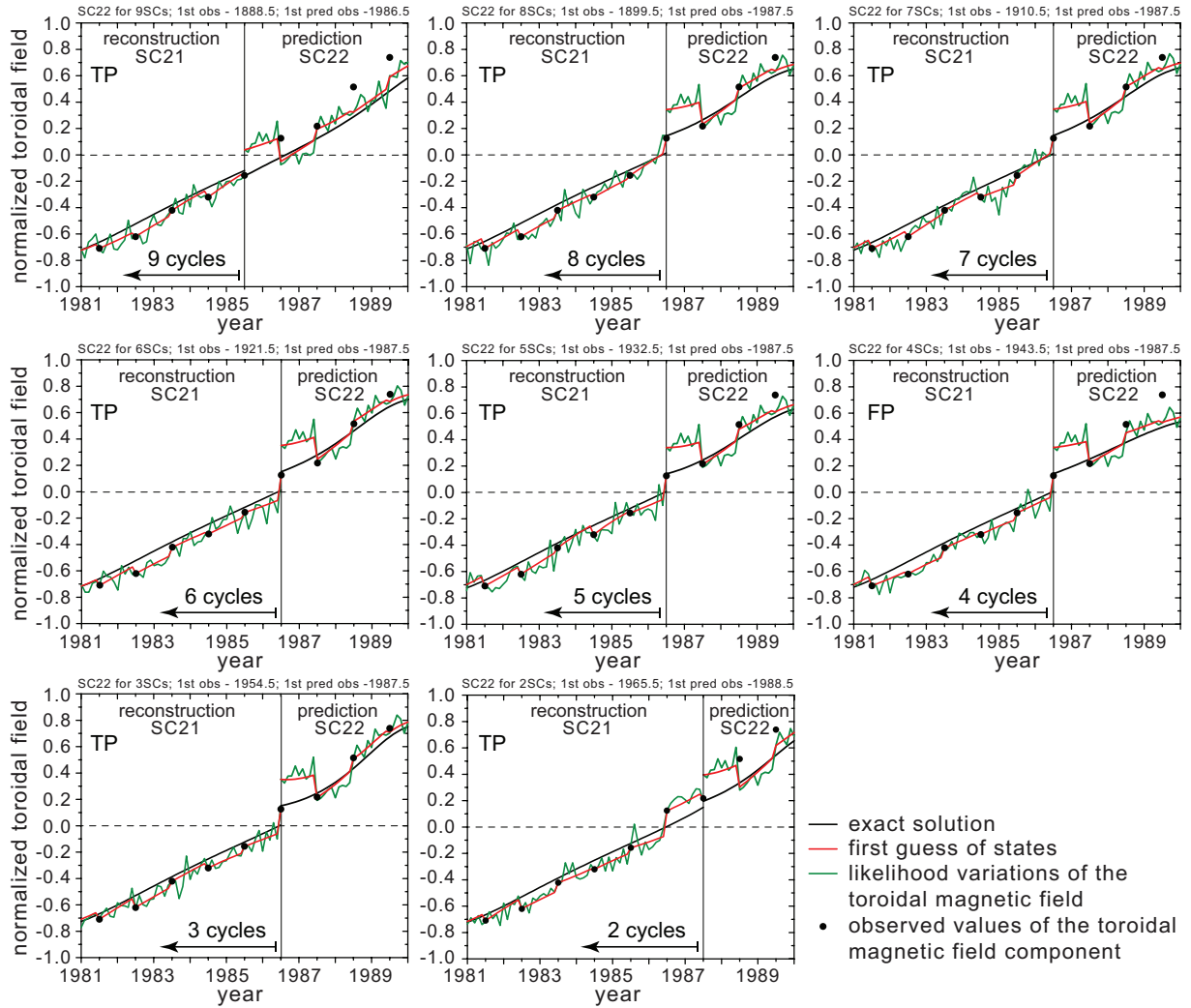


Fig. 9.— The same as in Figure 3 for Solar Cycle 22.

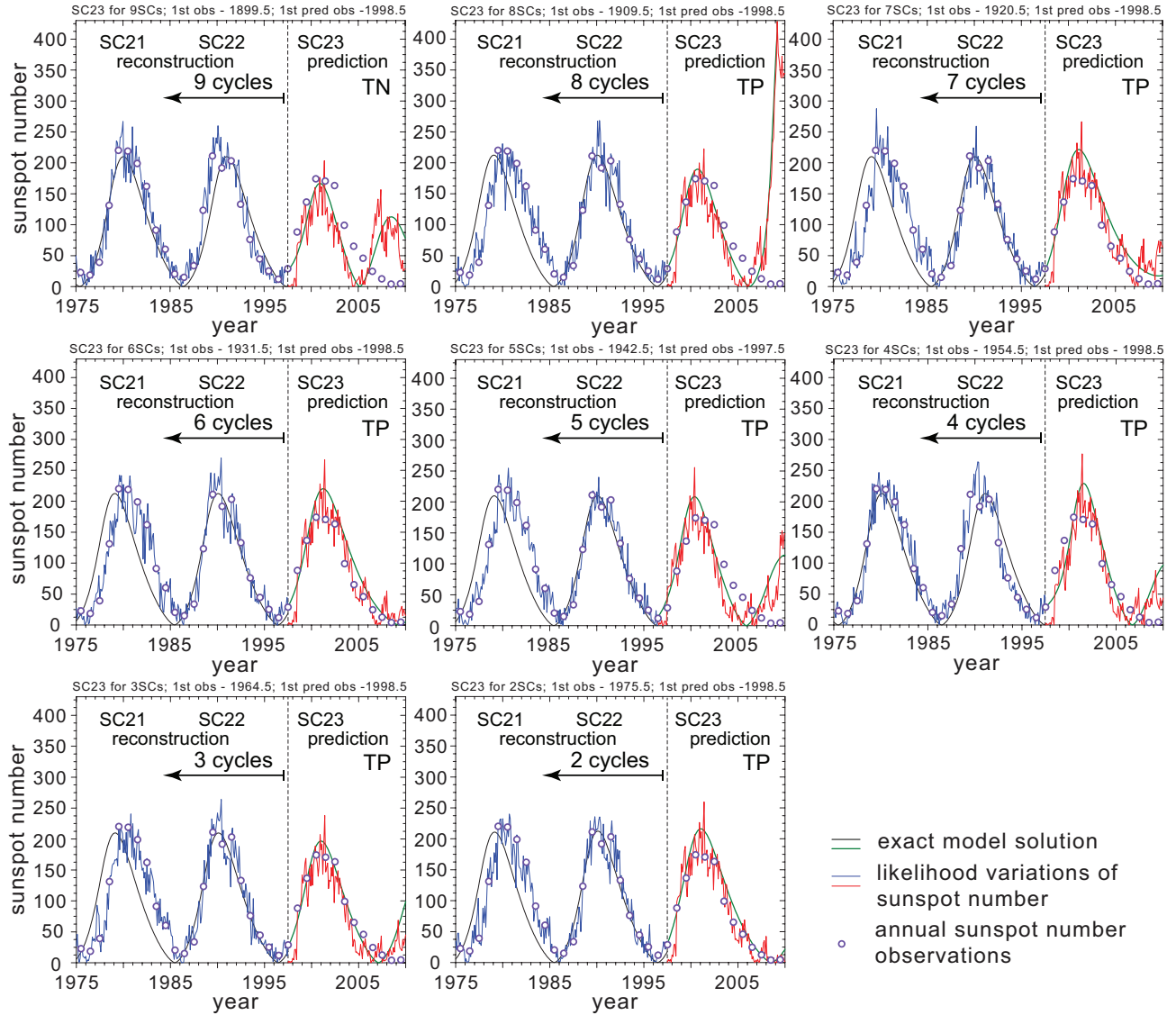


Fig. 10.— The same as in Figure 2 for Solar Cycle 23.

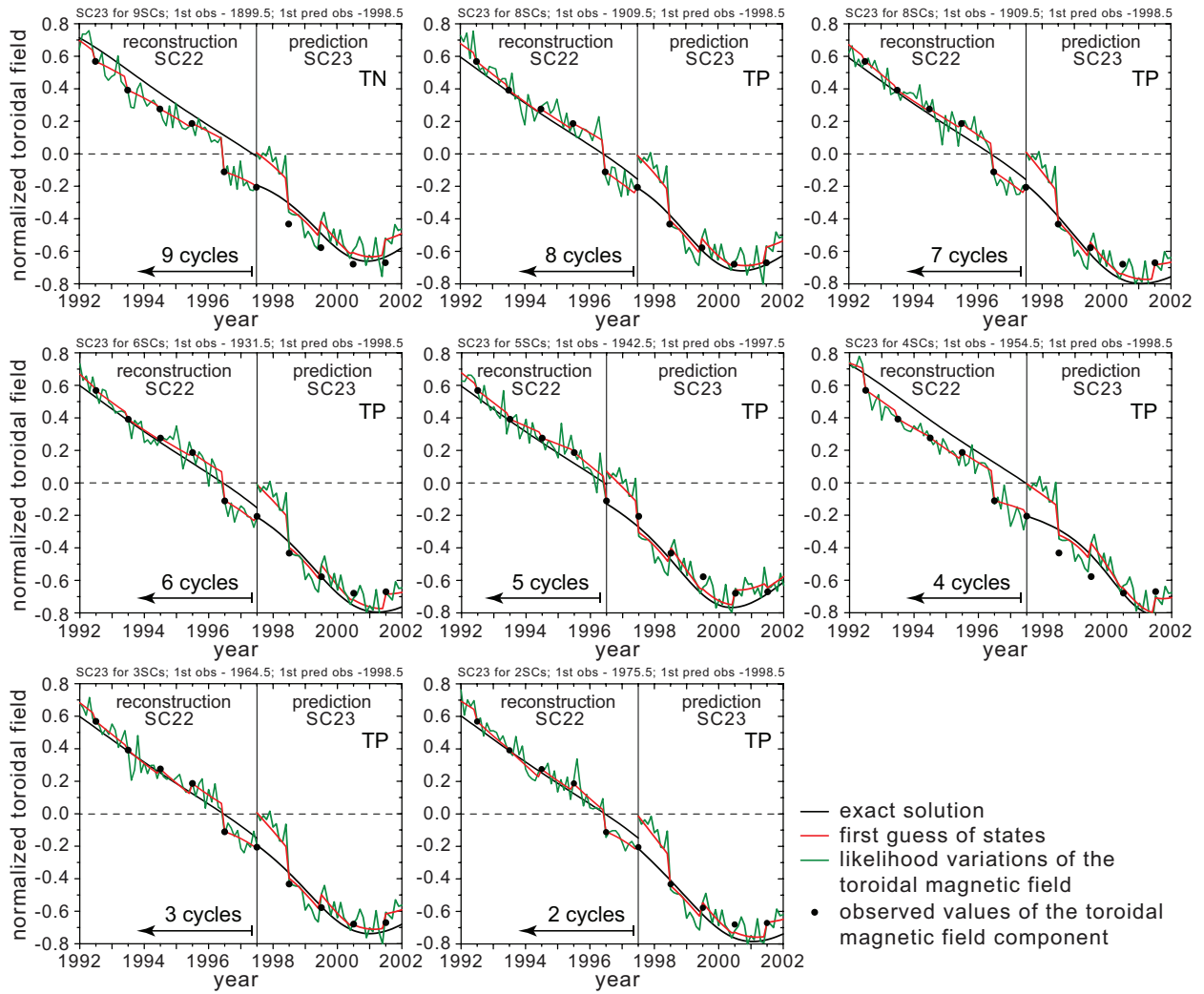


Fig. 11.— The same as in Figure 3 for Solar Cycle 23.

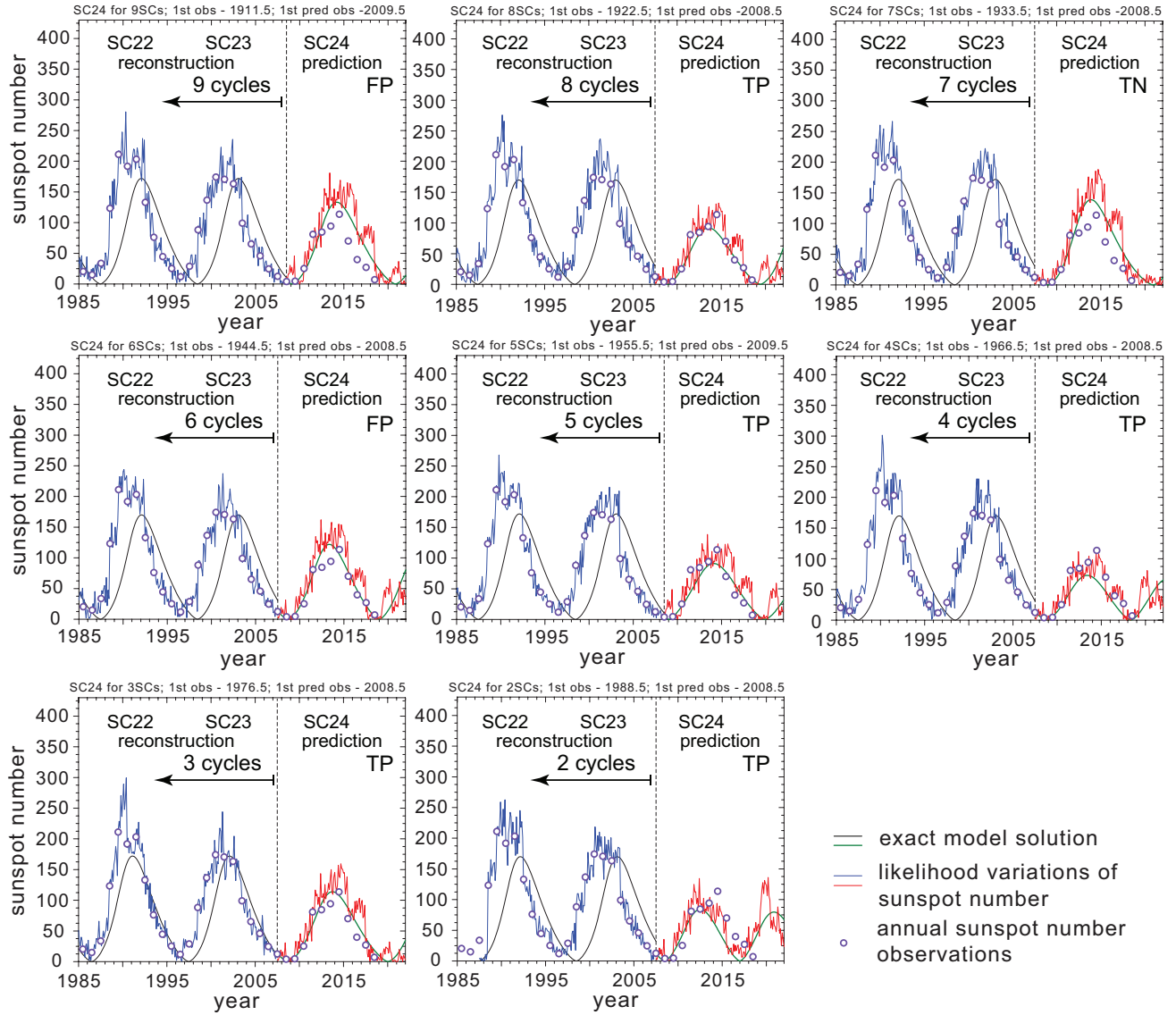


Fig. 12.— The same as in Figure 2 for Solar Cycle 24.

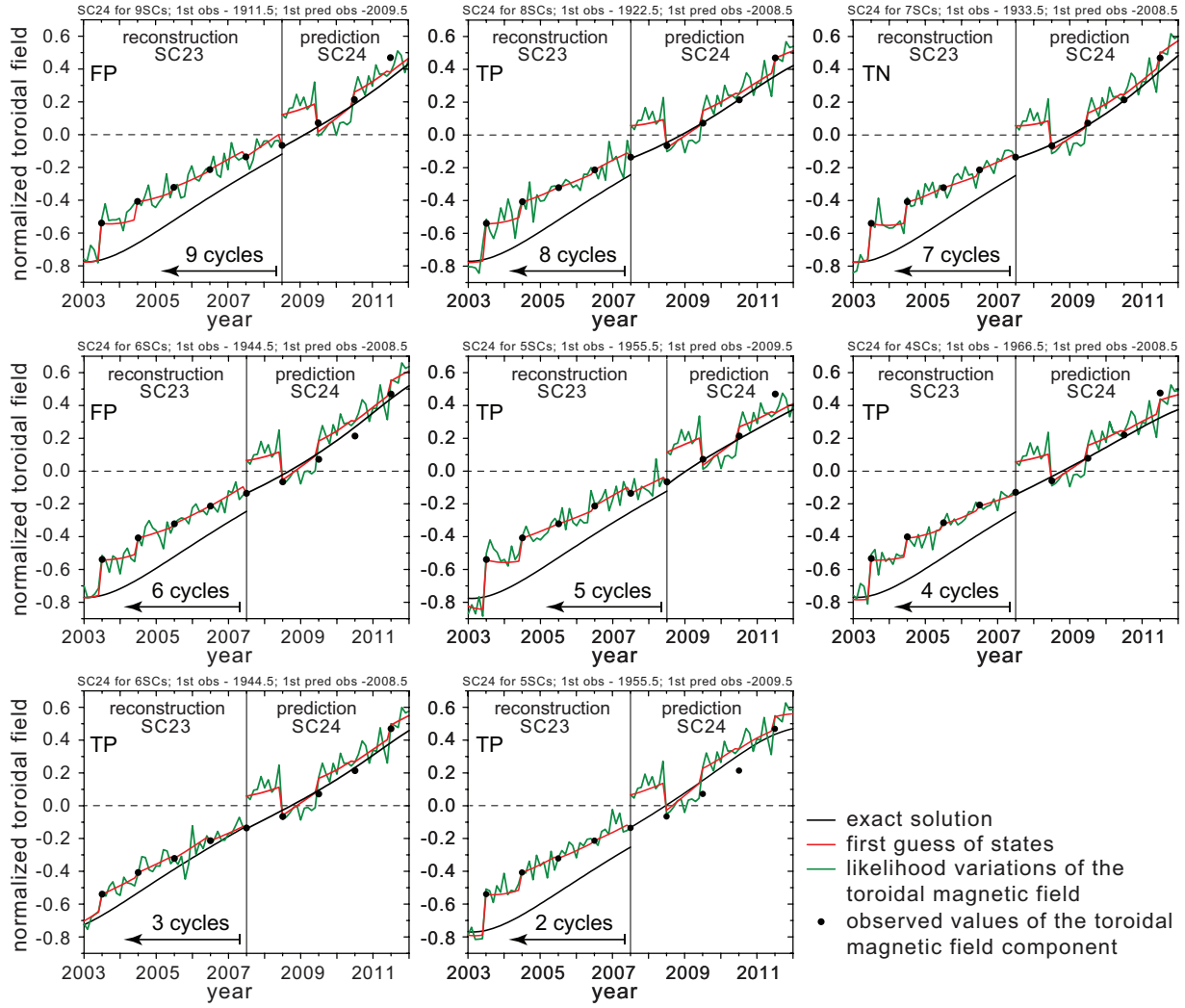


Fig. 13.— The same as in Figure 3 for Solar Cycle 24.